Step by step resolving the formation of dendritic crystal in solution: an observation against the classical model of one-by-one addition

Step by step resolving the formation of dendritic crystal in solution: an observation against the classical model of one-by-one addition

Y Wang[1, 2, 3], Y Li[1], L Liu[2], H Bai[1], S Zhao[1], R L Liu[1] and L Xu[1]

[1] School of Medicine, Xi'an Peihua University, Xi'an, 710125, P. R. China;
[2] Shaanxi Key Laboratory of Degradable Biomedical Materials, School of Chemical Engineering, Northwest University, Xi'an, 710069, P. R. China.

[3] E-mail: lanmao1998@163.com; wangya1@peihua.cn

Abstract. During crystallization, one-by-one addition of atomic species or nucleation-generated nanoparticles is widely considered to be the fundamental mode to construct advanced morphologies. However, due to a lack of approaches with high resolution and real-time tracing ability, the correctness of this conventional concept has never been verified in a complicated crystallization process, even including the simplest species--the formation of dendritic crystals. In this work, we successfully resolved the growth mechanism of dendritic KCl crystals in a thin water film by terminating the continuous crystallization at different stages. The results were quite against the conventional concept. For example, one-by-one aggregation of individual ions was unable to directly form a dendritic morphology, and nucleation-generated nanoparticles had been prearranged into dendritic configuration before they could attach one another. In summary, the crystallization was precisely self-controlled to follow several specific steps rather than the simple addition of building blocks.

1. Introduction

The crystal growth has been a central interest over the past decades in diverse scientific fields and a great progress has been made in crystal kinetics and the control of morphology [1-11]. Nevertheless, the essential understandings on how the basic building blocks are organized into advanced assemblies are still at the elementary level, not only including the complicated crystallizations but including the simplest species: the formation of dendritic crystal [12-16]. At present, both the classical and the non-classical theories take a view that constructing an advanced crystal is in fact a process of one-by-one aggregation of primary (atoms or ions) or derivative (nanoparticles) building blocks [2-9], which emphasizes on the growth continuity and interparticle attachment. However, as far as we know, it is difficult to verify that the crystal growth does follow the programmed theoretical modes, especially for the formation of dendritic crystal. One of the difficulties is that the building block is usually too small, and the growth rate is too fast. The most common means is using an optical microscope to real-time trace the crystallization, but the microscopic mechanisms remain inaccessible due to the low resolution of the optical microscopy. Other alternative methods with high resolution, such as transmission electron microscopy (TEM) [6], exhibits a potential to trace the crystal growth, but the monitoring area is usually too small to effectively trace a complete dynamic process.

As a solution to this challenge, tracing the crystal growth in a thin water film is promising to step by step resolve the whole crystallization process: the film can be fast dried to terminate the continuous

crystallization at different stages which can be easily resolved with a high resolution by atomic force microscopy (AFM) or scanning electron microscopy (SEM). In our previous work [17], a sandwich-like substrate was prepared to investigate a water nanofilm, which was formed by drying a drop of solution containing bovine serum albumin (BSA) and inorganic salt. During the drying process, BSA was enriched forming a solid skeleton and sandwiched between two thin layers of liquid containing inorganic ions. Here the ion-containing liquid layer is suitable for terminating the crystallization at different stages. As shown in Figure 1, focusing on the top water layer (Here only the top covered water layer within the sandwich structure is shown because it is close to the air side and hence easy for direct observations during the drying process compared to the other covered water layer at the bottom of the substrate), if the drying rate is high enough, the liquid layer is fast dried reaching absorption-desorption equilibrium of water vapor and thus is transformed into a water nanofilm in which nucleation-generated nanoparticles (NGNs) have not enough ability moving freely for further evolutions (Figure 1). A water nanofilm has been widely studied and confirmed to have ice-like structure and hence has very limited liquidity, which is helpful to terminate the assembly behaviours of NGNs (please refer to the Ref. [17] for details about the water nanofilm). By the logic, drying the sample under lower temperatures will decrease the dry rate, which increases the growth time and the degree of mobility freedom of NGNs during drying and allows them to form potential advanced assemblies. In general, lower drying rate corresponds to a later growth stage of NGNs, while higher drying rate corresponds to an earlier growth stage. In this work, we replaced Na_2CO_3 with KCl (referring to the previous work or the "Materials and methods" section for details) and terminated the crystallization of KCl at different stages by drying the BSA-KCl solution at a temperature range of 25-60 ℃(room relative humidity (RH) ~30-45%).

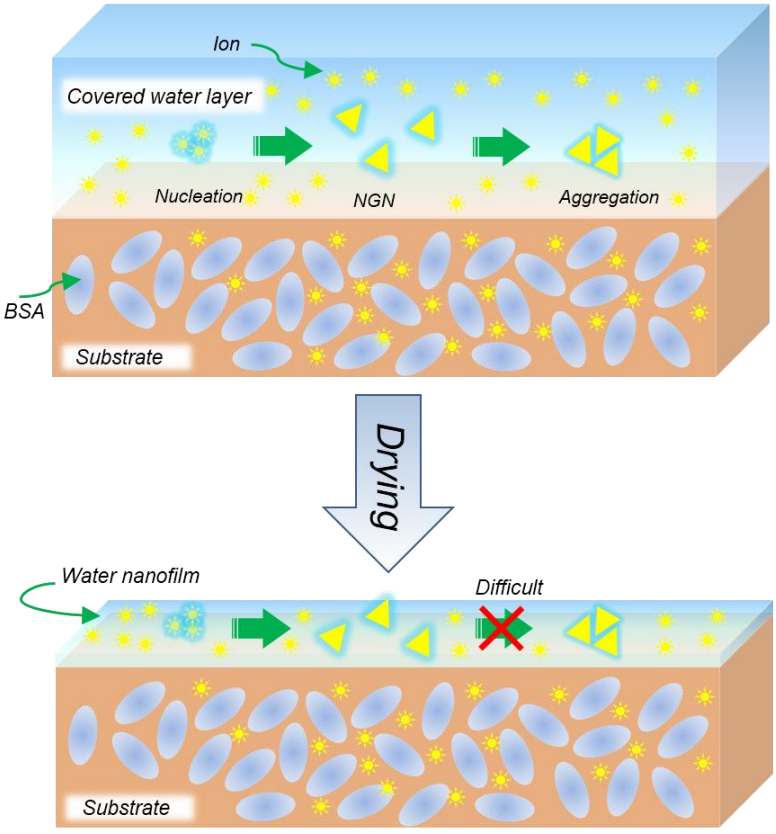

Figure 1. A schematic showing the termination mechanism during crystallization on the BSA-KCl substrate.

2. Materials and methods

2.1. Preparation of the BSA substrate

A KCl-containing BSA substrate was prepared first by referring to the following procedures: A mix of 75 mg BSA (purity >98%; Merck) and 15 mg of KCl was added to 1 mL of deionized water. Then, a droplet of the mixed solution (～10 μL) was added onto a silicon wafer (or electrically conductive glass) and dried under 25-60 ℃ on a hot stage for 1-2 h (the temperature depending on the control of crystallization rate).Thereafter, the dried substrate was observed within tens of minutes to 24 h with AFM or SEM at an appropriate RH (typically 30-45%) under room temperature.

2.2. AFM observations

A commercial AFM instrument (Dimension Icon, Bruker) was employed to image the crystallization process on the sample surface. In tapping mode imaging, a probe cantilever with a normal spring constant of ~40 N/m and a resonant frequency of ~300 kHz (RTESP, Veeco) was used, whereas in contact-mode imaging, cantilevers with normal spring constants of 0.06-0.58 N/m (NP-S10 or SNL-10, Bruker) were applied. All images were captured with a scan rate of 1 Hz (at room temperature).

2.3. SEM imaging

A commercial scanning electron microscope (Quanta600 FEG, FEI) was used to image the samples in low vacuum mode (90 Pa). For SEM imaging, the sample must be prepared on an electrically conductive medium such as an electrically conductive glass. During imaging, the accelerating voltage was set to 15-20 kV.

3. Results and discussions

The resulting evolution path of dendritic KCl crystal was concluded based on a descending dry rate (i.e., drying under decreasing hot stage temperatures). Initially, the sample was dried under 60 ℃ and the resulting substrate surface was flat without any detectable crystals (Figure 2A, the inset), which indicated that the crystallization might have been terminated at the nucleation stage (corresponding to the highest dry rate). If the sample was placed under ambient condition for water vapor adsorption, then many microcrystals (hundreds of nanometers in height) gradually occurred (Figure 2A& 2B) due to the diffusion and enrichment of inorganic ions in the water adlayer (nanoscale thickness) caused by the interfacial adsorption-desorption equilibrium of water vapor. In the nanofilm NGNs lost mobility but could keep growing into larger size and form nanoscale to microscale crystals by one-by-one addition of individual ions (Figure 2C). Obviously, if the dendritic crystal is only formed by one-by-one addition of atomic ions, its formation should be not easily limited by the water nanofilm. Here, however, we noted that no matter how processed the dried flat substrate (without crystals) with varied temperatures or RH conditions, no dendritic crystals could be achieved but instead, only discrete crystals were formed. For example, Figure 2A was observed hours ahead of Figure 2B, but they came from an identical sample. Compared the two SEM images, it can be clearly seen that the crystal number increased with time and the crystals became crowded. Note that in Figure 2B, a larger number of adjacent crystals were heavily coalesced with size growth, however, it was interesting that with the size and the number increasing, the coalesced crystals did not exhibit some assembly preference to evolve into advanced configurations but resulted in a littery particle map (Figure 2B). That is, once the NGNs are terminated at the nucleation stage and lose mobility, pure one-by-one addition of atomic species (ions) could only increase the size or number of the NGNs but is unable to make them evolve into advanced morphologies. Therefore, we infer that the dendritic configurations not only need one-by-one addition of ions, but also likely need the free mobility of NGNs.

At the next stage, it was found out that a large area of NGNs became closer to each other and arranged into a branching or linear configuration which would form the main outline of the final dendritic crystal (Figure 2D & 2E). It is worth noting that the well arrangement of NGNs took place at a distance beyond they could attach one another. The ‘attachment’ of microcrystals in Figure 2D (or

2E) was indeed caused by the addition of free ions after the 'termination' processing (Figure 2F). That is to say, the NGNs may occur first by classical one-by-one addition of ions during crystallization and then move closer to each other to form ordered configurations. Obviously, the non-contact prearrangement is against the conventional concept that crystallization is continuous process of one-by-one attachment of building blocks. Additionally, the microcrystals within the linear configuration were smaller than the surrounding ones, which means that once an NGN was employed for advanced assembly, the growth rate of itself would be significantly reduced.

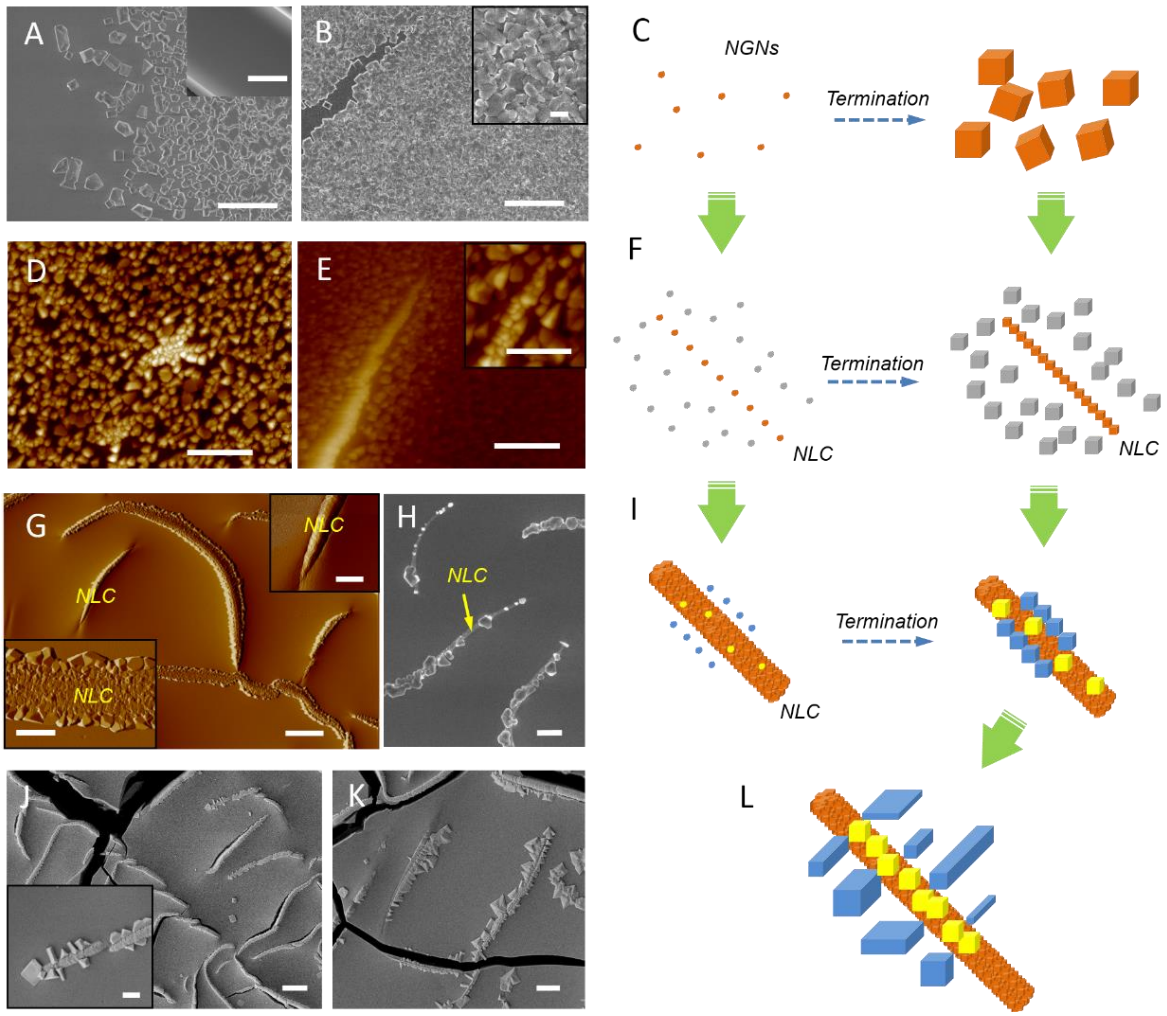

Figure 2. The left column: typical AFM or SEM images captured during the formation of dendritic KCl crystal based on roughly decreasing drying rate. (A, B, H, J, K) are SEM images; (D, E, G) are AFM images. The inset of (A) is the initial morphology of the sample dried under 60 ℃. (A) and (B) show the how the surface morphology of the sample changed with time, (A) was observed hours ahead of (B). (D&E), (G&H) or (J&K) came from two different areas of a sample terminated at a certain stage. All insets are magnified views except the inset of (A). The right column: schematic diagram to demonstrate the morphology formation of the corresponding left column. Scale bars: 10 μm for (A) (and the inset), (B), (J) and (K); 1 μm for (D), (E), insets of (B) and (G); 400 nm for the inset of (E); 2 μm for (H) and inset of (J); 5 μm for (G).

With respect to the third stage, the linear configuration became a compact needle-like crystal (NLC) (Figure 2G, 2H & 2I) so that it was difficult to distinguish individual microcrystals (evolving from NGNs). However, on both sides (indicated with blue blocks in Figure 2I) and the top (indicated with

yellow blocks in Figure 2I) of the NLC, large-size microcrystals appeared in sequence, which was in fact ready for subsequent branching. Here we emphasized that the bilateral microcrystals appeared first and the top microcrystals second (Figure 2H & 2I) because this preference directly lead to the two- dimensional branch-like morphology. Additionally, it could be inferred that the whole area of NGNs at this stage were employed to build the NLC s as the surrounding microcrystals were seldom observed. We also noted that the addition of NGNs onto the top of NLC did not follow the conventional 'one-by-one addition' style but instead, they were randomly attached to NLC using NLC itself as the template (Figure 2H). When it came to the final stage, bilateral microcrystals kept growing by addition of individual ions and formed branches (Figure 2J, 2K & 2L). Here the branches were individual single crystals instead of NLC due to the limited number of ions in the liquid layer. That is, if the ion concentration was high enough, more NGNs would be generated to form more branches NLCs following the abovementioned pathway and resulted in a self-similar dendritic morphology.

4. Summary

In summary, the detailed growth mechanism of dendritic KCl crystal was successfully resolved by terminating the continuous crystallization at different stages. The results were largely against the conventional concept, which were concluded as follows. Firstly, one-by-one addition of individual ions was unable to form a dendritic morphology, in other words, NGNs were needed to be generated for advanced construction. Secondly, the in-situ coalescence of immobile NGNs was also unbale to form ordered configurations. Thirdly, NGNs needed be prearranged into the specific configuration without interparticle attachment in a fluidic environment to construct the dendritic style, suggesting that long- range interparticle interactions might be probably the determinant of complicated morphologies. Fourthly, the NLC itself could serve as a template for the discrete attachment of NGNs. Finally, the formation of dendritic morphology followed specific steps strictly, which means that there might be a programmed termination mechanism at each step.

Acknowledgements

The work was financially supported by the National Natural Science Foundation of China (21277210, 21476182) and the Scientific Research Starting Foundation of Xi'an Peihua University.

References

[1] Feigelson R S 2004 *50 years progress in crystal growth* (London: Elsevier)
[2] Miszta K, de Graaf J, Bertoni G, Dorfs D, Brescia R, Marras S, Ceseracciu L, Cingolani R, van Roij R, Dijkstra M and Manna L 2011 *Nat. Mater.* **10** 872-6
[3] Penn R L 2004 *J. Phys. Chem. B* **108** 12707-12
[4] Ribeiro C, Lee E J, Longo E and Leite E R 2005 *ChemPhysChem* **6** 690-6
[5] Zhang J, Lin Z, Lan Y, Ren G, Chen D, Huang F and Hong M 2006 *J. Am. Chem. Soc.* **128** 12981-7
[6] Li D, Nielsen M H, Lee J R, Frandsen C, Banfield J F and De Yoreo J J 2012 *Science* **336** 1014-8.
[7] Cölfen H and Mann S 2003 *Angew. Chem. Int. Edit* **42** 2350-65
[8] Niederberger and Cölfen H 2006 *Phys. Chem. Chem. Phys.* **8** 3271-87
[9] Zhang Z, Sun H, Shao X, Li D, Yu H and Han M 2005 *Adv. Mater.* **17** 42-7
[10] Lim B, Jiang M, Tao J, Camargo P H, Zhu Y and Xia Y 2009 *Adv. Funct. Mater.* **19** 189-200
[11] Jun Y W, Lee J H, Choi J S and Cheon J 2005 *J. Phys. Chem. B* **109** 14795-806
[12] Dougherty A, Kaplan P D and Gollub J P 1987 *Phys. Rev. Lett.* **58** 1652-5
[13] Kessler D A, Koplik J and Levine H 1986 *Phys. Rev. A* **33** 3352-7
[14] Glicksman M E and Lupulescu A O 2004 *J. Cryst. Growth.* **264** 541-9
[15] Glicksman M E, Schaefer R J and Ayers J D 1976 *Metall. Trans. A* **7** 1747-59
[16] Sethian J A and Straint J 1992 *J. Comput. Phys.* **98** 231-53
[17] Wang Y, Duan Z and Fan D 2013 *Sci. Rep.***3** 3505